

EFFECT OF SEISMIC DEGHOSTING ON THE PREDICTED P-IMPEDANCE
CONTRAST

TAN KAH SING

A project report submitted in partial fulfillment of the
requirements for the award of the degree of
Master of Petroleum Engineering

Faculty of Chemical and Energy Engineering
Universiti Teknologi Malaysia

JANUARY 2018

To my beloved mother and father

ACKNOWLEDGEMENT

In preparing this thesis, I was in contact with many people, researchers and academicians. They have contributed towards my understanding and thoughts. In particular, I wish to express my sincere appreciation to my main thesis supervisor, Dr. Muhammad Akhmal Muhammad Sidek, for encouragement, guidance, critics and friendship. Without his continued support and interest, this thesis would not have been the same as presented here.

My fellow postgraduate students and course mates should also be recognized for their support. My sincere appreciation also extends to all my colleagues, especially Mr. Gan Wei Di, who has provided assistance at various occasions. Their views and tips are useful indeed. Unfortunately, it is not possible to list all of them in this limited space. I am also grateful to all my family members who have been supportive during the preparation of this thesis.

Last but not least, I would like to thank my manager, Mr. Gunaseelan Nandan Cumarana, who helped me to obtain permission to use seismic data of Vulcan sub-basin and DownUnder Geosolutions (DUG) proprietary Insight software to process the seismic data and run seismic inversion algorithm. A token of appreciation is also given to Department of Mines and Petroleum, Western Australia to provide the well logs for the 3 wells located inside Vulcan sub-basin seismic data.

ABSTRACT

The purpose of this study is to investigate the effectiveness of different deghosting algorithm as well as the effect of sea state parameter on the deghosting result. Subsequently, the predicted p-impedance contrast from best deghosted result and recorded p-impedance contrast from well logs are compared. Seismic data in Vulcan Sub-basin is being processed with the same sequences except for deghosting process. DUG Insight seismic processing software was used in this study. Initially, different deghosting algorithm of deterministic and adaptive deghosting is applied on seismic data. After choosing a better deghosting algorithm, sea state of 0.2, 0.4, 0.6, 0.8 and 1 are applied on the similar seismic data. The deghosting result is examined via seismic images, amplitude spectra, autocorrelation and p-impedance contrast obtained from seismic inversion. The best deghosted result is then feed into seismic inversion module together with well logs at different well locations. It is found out that adaptive deghosting algorithm provides better result compared to deterministic deghosting because adaptive deghosting handles variation of ghost parameters across seismic data better. Sea state parameter heavily depends on the condition of seismic data. The cleaner the seismic data, the higher the sea state parameter. In this study, maximum seastate of 1.0 is chosen due to noiseless seismic data. Last but not least, the predicted p-impedance contrast from seismic inversion gives mediocre results from the perspective of accuracy. However, it gives superb result in identifying hydrocarbon-bearing layers. The deghosting and seismic inversion study is one of the first in Vulcan Sub-basin which act as yardstick for further work in this region.

ABSTRAK

Tujuan kajian ini adalah untuk mengkaji kesan algoritma “nyahhantu” dan nilai “keadaan lautan” yang berbeza ke atas keputusan “nyahhantu”. Kemudian, kontras p-impedans yang dijangka daripada keputusan “nyahhantu” yang terbaik akan dibandingkan dengan kontras p-impedans yang dicatat dalam log telaga. Data seismik di sub-lembangan Vulcan diproses dengan urutan yang sama selain proses “nyahhantu”. Perisian pemprosesan seismik “DUG Insight” digunakan dalam kajian ini. Mula-mula, algoritma “nyahhantu” deterministik dan adaptasi yang berbeza digunakan atas data seismik. Selepas memilih algoritma “nyahhantu” yang lebih baik, “keadaan lautan” daripada 0.2, 0.4, 0.6, 0.8 hingga 1 digunakan atas data seismik yang sama. Keputusan “nyahhantu” diperiksa melalui imej seismik, spektra amplitud, autokorelasi dan kontras p-impedans daripada penyongsangan seismik. Keputusan “nyahhantu” yang terbaik dimasukkan dalam modul penyongsangan seismik bersama-sama dengan log telaga di kedudukan telaga yang berbeza. Adalah didapati bahawa algoritma “nyahhantu” adaptasi memberi keputusan yang lebih baik berbanding dengan “nyahhantu” deterministik kerana “nyahhantu” adaptasi mengendali variasi nilai “hantu” dalam data seismik dengan lebih baik. Nilai “keadaan lautan” sangat bergantung kepada keadaan data seismik. Semakin bersih data seismik, semakin tinggi nilai “keadaan lautan”. Dalam kajian ini, nilai tertinggi “keadaan lautan” sebanyak 1.0 dipilih kerana data seismik sangat bersih. Akhir sekali, kontras p-impedans yang dijangka daripada penyongsangan seismik memberi keputusan yang sederhana dari segi kejituan. Walau bagaimanapun, penyongsangan seismic memberi keputusan yang baik dalam mengesan lapisan hidrokarbon. Kajian “nyahhantu” dan penyongsangan seismik adalah antara yang pertama di sub-lembangan Vulcan yang dapat dijadikan kayu ukur bagi kajian seterusnya pada masa depan.

TABLE OF CONTENTS

| CHAPTER | TITLE | PAGE |
|----------|---------------------------|----------|
| | DECLARATION | iii |
| | DEDICATION | v |
| | ACKNOWLEDGEMENT | vii |
| | ABSTRACT | viii |
| | ABSTRAK | ix |
| | TABLE OF CONTENTS | x |
| | LIST OF TABLES | xiii |
| | LIST OF FIGURES | xiv |
| | LIST OF SYMBOLS | xvii |
| 1 | INTRODUCTION | 1 |
| | 1.1 Introduction | 1 |
| | 1.2 Statement of Problem | 4 |
| | 1.3 Objective | 9 |
| | 1.4 Hypotheses | 10 |
| | 1.5 Scope | 10 |
| | 1.6 Significance of Study | 11 |

| | | |
|----------|--|-----------|
| 2 | LITERATURE REVIEW | 13 |
| 2.1 | Seismic Deghosting | 13 |
| 2.1.1 | Introduction | 13 |
| 2.1.2 | Acquisition Deghosting | 13 |
| 2.1.2.1 | Acquisition Source Deghosting | 13 |
| 2.1.2.2 | Acquisition Receiver Deghosting | 15 |
| 2.1.3 | Algorithm Deghosting | 19 |
| 2.1.3.1 | Introduction | 19 |
| 2.1.3.2 | Deterministic Deghosting | 19 |
| 2.1.3.3 | Disadvantage of Deterministic Deghosting | 24 |
| 2.1.3.4 | Adaptive Deghosting | 25 |
| 2.1.4 | Seismic Deghosting Technology by Processing Companies | 29 |
| 2.1.5 | Advantages of Seismic Deghosting | 30 |
| 2.2 | Seismic Inversion | 33 |
| 2.2.1 | Introduction | 33 |
| 2.2.2 | Input Data to Seismic Inversion | 35 |
| 2.2.3 | Methodologies and Applications of Seismic Inversion | 36 |
| 2.3 | Well Logging | 39 |
| 2.3.1 | Introduction | 39 |
| 2.3.2 | Density Logging | 39 |
| 2.3.3 | Sonic Logging | 41 |
| 2.4 | Vulcan Sub-basin | 43 |
| 2.4.1 | Introduction and Geological Settings | 43 |
| 2.4.2 | Previous Work Done in Vulcan Sub-basin | 44 |
| 3 | RESEARCH METHODOLOGY | 49 |
| 3.1 | Introduction | 49 |

| | | |
|----------|--|-----------|
| 3.2 | Details of Research Sequences | 52 |
| 4 | RESULTS AND DISCUSSIONS | 55 |
| 4.1 | Introduction | 55 |
| 4.2 | Deghosting Algorithm Testing Results | 57 |
| 4.3 | Deghosting Parameter (Sea State) Testing Results | 65 |
| 4.4 | Comparison between Predicted and Recorded P-impedance Contrast | 79 |
| 5 | CONCLUSIONS AND RECOMMENDATIONS | 87 |
| 5.1 | Conclusions | 87 |
| 5.2 | Recommendations | 88 |
| | REFERENCES | 89 |

LIST OF TABLES

| TABLE NO. | TITLE | PAGE |
|------------------|---|-------------|
| 2.1 | Important information regarding to Vulcan Sub-basin petroleum system elements | 44 |
| 3.1 | Steps involved in research | 50 |

LIST OF FIGURES

| FIGURE NO. | TITLE | PAGE |
|------------|---|------|
| 1.1 | Map view and side view of marine seismic acquisition | 2 |
| 1.2 | Illustration of different type of ghosts | 5 |
| 1.3 | Mirror source and receiver models | 7 |
| 1.4 | Ghost notches introduced by different source or receiver Depths | 9 |
| 2.1 | Source configuration of Delta 3 source array | 15 |
| 2.2 | Various hydrophones configuration to overcome ghost | 16 |
| 2.3 | Illustration of variable depth streamer configuration | 16 |
| 2.4 | Illustration of τ - p transform | 26 |
| 2.5 | Various paths taken by gamma ray in formation | 40 |
| 2.6 | Types of waves being recorded by sonic log | 42 |
| 2.7 | Location of Vulcan Sub-basin and the seismic surveys and wells available in that area | 46 |
| 2.8 | Top Permian TWT of Vulcan Sub-basin mega survey | 47 |
| 3.1 | Location of Cygnus 3D seismic survey | 51 |
| 3.2 | Detailed coverage of Cygnus 3D survey together with wells available | 52 |
| 4.1 | Arbitrary line drawn across 899km ² seismic survey | 56 |
| 4.2 | Seismic data with ghost along arbitrary line together with gamma ray logs of 3 wells | 56 |

| | | |
|------|---|----|
| 4.3 | Input seismic data before deghosting | 58 |
| 4.4 | Output seismic data after deterministic deghosting | 58 |
| 4.5 | Output seismic data after adaptive deghosting | 59 |
| 4.6 | Zoomed input seismic data before deghosting | 60 |
| 4.7 | Zoomed output seismic data after deterministic deghosting | 60 |
| 4.8 | Zoomed output seismic data after adaptive deghosting | 61 |
| 4.9 | Portion of seismic data confined by red rectangle to compute frequency spectrum | 62 |
| 4.10 | Amplitude spectrum (dB scale) for seismic data before and after deghosting using different deghosting algorithm | 62 |
| 4.11 | Predicted p-impedance contrasts at Wisteria-1 well for deterministic and adaptive deghosting results together with p-impedance contrast recorded by well logs | 65 |
| 4.12 | Seismic data before deghosting | 66 |
| 4.13 | Seismic data after deghosting with sea state 0.2 | 66 |
| 4.14 | Seismic data after deghosting with sea state 0.4 | 67 |
| 4.15 | Seismic data after deghosting with sea state 0.6 | 67 |
| 4.16 | Seismic data after deghosting with sea state 0.8 | 68 |
| 4.17 | Seismic data after deghosting with sea state 1.0 | 68 |
| 4.18 | Zoomed seismic data before deghosting | 69 |
| 4.19 | Zoomed seismic data after deghosting with sea state 0.2 | 70 |
| 4.20 | Zoomed seismic data after deghosting with sea state 0.4 | 70 |
| 4.21 | Zoomed seismic data after deghosting with sea state 0.6 | 71 |
| 4.22 | Zoomed seismic data after deghosting with sea state 0.8 | 71 |
| 4.23 | Zoomed seismic data after deghosting with sea state 1.0 | 72 |
| 4.24 | Amplitude spectrum (dB scale) for seismic data before and after deghosting with different seastate | 73 |
| 4.25 | Autocorrelation of seismic data before deghosting | 75 |
| 4.26 | Autocorrelation of seismic data after deghosting with seastate 0.2 | 75 |
| 4.27 | Autocorrelation of seismic data after deghosting with seastate | |

| | | |
|------|---|----|
| | 0.4 | 76 |
| 4.28 | Autocorrelation of seismic data after deghosting with seastate | |
| | 0.6 | 76 |
| 4.29 | Autocorrelation of seismic data after deghosting with seastate | |
| | 0.8 | 77 |
| 4.30 | Autocorrelation of seismic data after deghosting with seastate | |
| | 1.0 | 77 |
| 4.31 | Predicted p-impedance contrasts at Wisteria-1 well for deghosting input and seastate 1.0 deghosting output together with p-impedance contrast recorded by well logs | 78 |
| 4.32 | Predicted and recorded p-impedance contrasts at Wisteria-1 well | 80 |
| 4.33 | Predicted and recorded p-impedance contrasts at Birch-1ST1 well | 80 |
| 4.34 | Predicted and recorded p-impedance contrasts at Puffin-6 well | 81 |
| 4.35 | Well tie result at Wisteria-1 well | 83 |
| 4.36 | Well tie result at Birch-1ST1 well | 83 |
| 4.37 | Well tie result at Puffin-6 well | 84 |
| 4.38 | P-impedance values overlain with entire seismic data along arbitrary line | 85 |
| 4.39 | P-impedance values overlain with zoomed seismic data along arbitrary line | 86 |

LIST OF SYMBOLS

| | | |
|----------|---|-----------------------------------|
| t_r | - | Travel lag time of receiver ghost |
| t_s | - | Travel lag time of source ghost |
| Z_g | - | Source or receiver depth |
| c | - | Water velocity |
| ρ | - | Density |
| V_z | - | Vertical particle velocity |
| ω | - | Angular frequency |
| V_z | - | Vertical particle velocity |
| G | - | Ghost operator |
| U | - | Ideal seismic data without ghost |
| τ | - | Zero offset intercepting time |
| p | - | Slowness parameter |
| f | - | Frequency |
| V_p | - | Compressional velocity |
| DT | - | Sonic slowness |
| TWT | - | Two way time |
| dB | - | decibel |
| V_p | - | primary wave (p-wave) velocity |

CHAPTER 1

INTRODUCTION

1.1 Introduction

Since 19th century, hydrocarbon such as oil and gas has become major energy source in the world to propagate the advance of human civilization. However, hydrocarbon is a non-renewable energy and its amount is depleting due to continuous extraction. Regions with easily-extracted hydrocarbon such as barren land and shallow sea are running out of economically feasible hydrocarbon, thus forcing human to explore new and challenging terrain such as deep sea to search for more oil and gas. Marine region on Earth has abundant prospect for hydrocarbon since it covers 70 percent of Earth's surface and has numerous discovered or undiscovered basins that accumulate huge hydrocarbon reserves. Examples are Taranaki Basin and Carnarvon Basin in New Zealand and Australia respectively.

To extract hydrocarbon from challenging marine environment, proper understanding of the geological structure of the prospect area is very important. This is because hydrocarbon exploration stage, especially confirmation and development wells drilling, is very expensive and cannot be carried out in region without prospect. Till now, seismic survey is the single most powerful technique to obtain information on geological structure of marine environment. The energy source for seismic survey is powerful rechargeable air guns that fire high energy sound pulses continuously onto the seabed. The air guns are designed to create broadband sound pulses that range from low to high frequencies in order to capture all geological structures subsurface, ranging from thin

sand layers to thick channels. The frequency can reach as low as 2Hz and highest about 250Hz. The air guns are towed behind seismic vessel together with streamers that are electrically connected to the seismic vessel. The streamers are equipped with piezoelectric hydrophones to record the sound pulses that travel beneath the subsurface and penetrate back to the sea water. The recording interval of the hydrophones is 2ms, which is equivalent to Nyquist frequency of 250Hz, so that the frequencies generated by the air guns can be recorded fully. Typically, air guns and hydrophones are placed about 10m and 15m below the sea level to reduce the recording of swell noise at the sea surface. There are different configurations of air guns and hydrophones to maximize the recorded signals reflected from subsurface, for instance multi-air guns Wide-Azimuth acquisition to image salt dome at Gulf of Mexico. Figure 1.1 shows the typical setup of marine seismic acquisition. The paravanes are used to stabilize the air guns and streamers, thus maintaining them at correct position during acquisition.

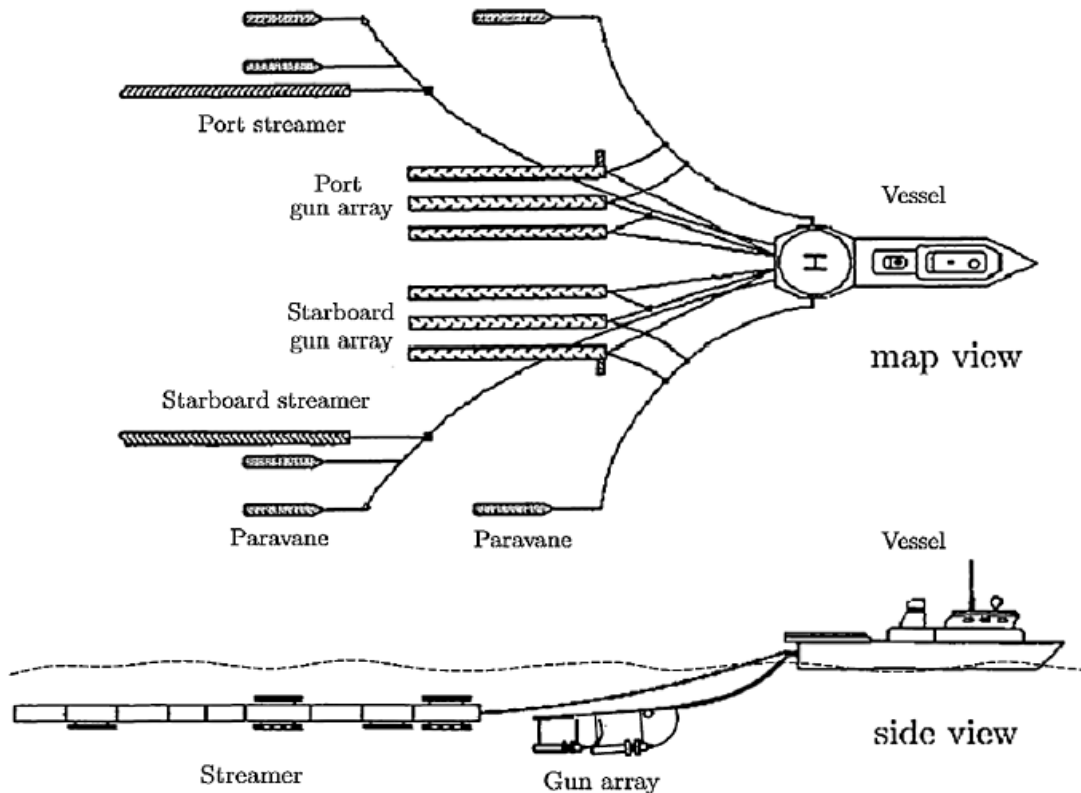


Figure 1.1 Map view and side view of marine seismic acquisition [1]

After the offshore seismic data acquisition, seismic data stored in the form of field tapes are being transported onshore for further processing. The two main objectives of seismic processing are as follow:

1. Attenuate the noises and unwanted signals embedded in seismic data so that only primary reflections are retained. Primary reflections are defined as signals that only reflect once below the sea level. Noises include swell noise caused by rough sea, linear noise originated from direct arrival of sound pulses of air guns to hydrophones without being reflected subsurface and interference noise due to spurious noise from nearby sailing ships. Unwanted signals include multiples and ghosts. Multiples are sound pulses that reflect more than one time below sea level while concept of ghosts will be discussed in depth later.
2. Obtain true image of the subsurface via migration. Seismic data are recorded as scattered waves that are reflected from subsurface anomalies such as fault, dipping reflectors and salt dome before migration. Migration relocates those scattered waves temporally and spatially to correct subsurface locations, thus giving an accurate subsurface image. The key to migration is accurate subsurface velocity which is obtained from seismic data with its noises and unwanted signals properly attenuated. Hence, elimination of noises and unwanted signals is crucial in determining the success of seismic processing.

The output of seismic processing, usually in the form of stacks, migrated gathers and velocities, is used by geophysicists to interpret the geological structures quantitatively. Direct hydrocarbon indicators (DHI) such as bright flat spots and polarity or impedance reversals are identified on seismic stacks to ensure presence of hydrocarbon. Next, amplitude versus offset (AVO) rotations study is carried out to quantify the probability of presence of hydrocarbon reserves at particular location and depth. Exploration well is then drilled at the location with the highest probability of hydrocarbon presence. Hence, the success of exploration well drilling heavily depends on the effectiveness of seismic processing sequences as mentioned above.

While drilling exploration well, well logs are taken to obtain further information of the subsurface such as lithology and fluid content. Well log data and seismic data

complement with each other because seismic data has good lateral resolution but poor vertical resolution (about 20m) while well log data has poor lateral resolution but good vertical resolution (about 1m). Examples of well logs taken are density log, velocity log and spontaneous potential (SP) log. From the well logs, fundamental information of the lithology and fluid such as bulk modulus, shear modulus and density can be known. Those well logs information together with seismic data are then utilized again by the geophysicists to carry out better quantitative interpretation (QI) study on the regional subsurface. The parameter that links well logs and seismic data together in QI study is p-impedance. P-impedance is derived from exploration well logs by multiplying density with compressional velocity of the medium. On the other hand, p-impedance is obtained from seismic data via seismic inversion with the exploration well logs information as extra constraint so that results of seismic inversion ties with the subsurface lithology.

P-impedance is of utter importance in hydrocarbon exploration because it is the only parameter that can identify lithology and fluid content due to the fact that each medium has distinct p-impedance value. The main objective of QI study in this stage is to predict lithology and fluid content away from exploration well accurately by using p-impedance contrast. P-impedance contrast study is a good tool to differentiate between hydrocarbon layers and non-producing layers. This study is economically important because hydrocarbon reserves cover a vast area and it is impossible to drill abundant high-cost exploration wells to evaluate the presence of hydrocarbon. Hence, it is anticipated that all the information related to subsurface can be known with only seismic data and exploration well available, thus minimizing the hydrocarbon exploration cost. To achieve this noble objective, the quality of seismic data processing is again very important to ensure that the subsurface information can be known by seismic data-driven approach instead of well-driven approach.

1.2 Statement of Problem

Since all the hydrocarbon exploration stages, ranging from quantitative interpretation to exploration well drilling, emphasize on the importance of seismic data processing, it is ideal to develop more robust algorithm to tackle unwanted signals, especially ghost in seismic data. Ghost attenuation receives attention from geophysics community in the past decade thanks to the advent of new deghosting algorithm. Ghost occurs due to the reflection of the air gun sound pulses from the sea surface because both the air guns and hydrophones are towed below sea surface to reduce the swell effect on signal. There are three types of ghosts, namely receiver ghost, source ghost and both source and receiver ghost. Figure 1.2 illustrates the different types of ghosts present. In the first row of Figure 1.2, red star is the air gun while blue triangle is the receiver or hydrophone. No ghost scenario is ideal case where only primary reflection is recorded and there is no reflection from sea surface. Primary reflection is recorded as the pressure variation of sound pulses inside water column. Receiver ghost occurs when upgoing wave from subsurface is reflected from sea surface before travelling to receiver. On the other hand, source ghost occurs when wave from air gun is reflected from sea surface before travelling downwards to subsurface. Both source and receiver ghosts occur when the raypath which causes source and receiver ghost occur simultaneously. Ghost occurs due to the large acoustic impedance (density and velocity) difference between seawater and air interface that induces strong and negative reflection downwards.

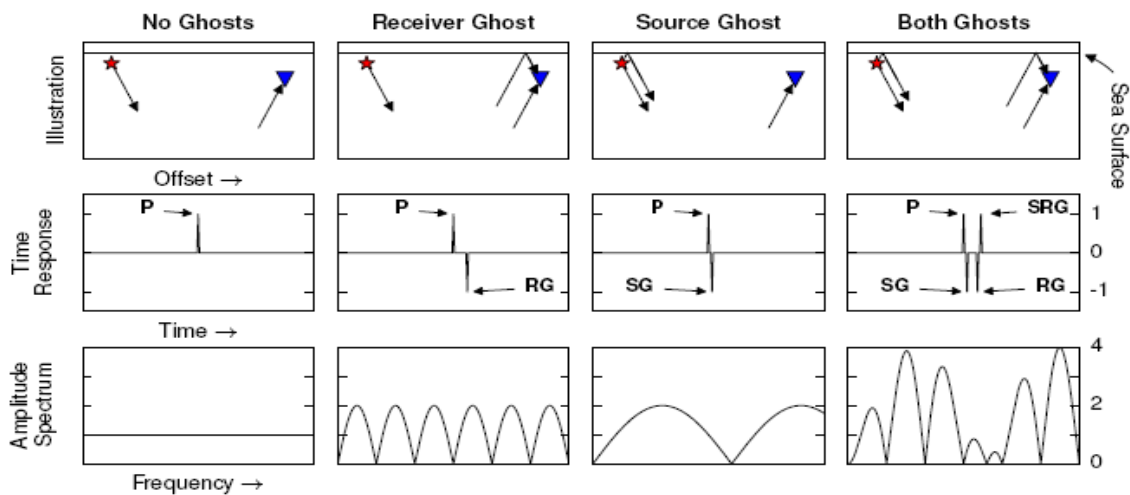


Figure 1.2 Illustration of different type of ghosts. P, RG, SG and SRG are primary, receiver ghost, source ghost and source-receiver ghost respectively. [2]

The major disadvantages of ghost embedded in seismic data are as follow:

1. Distortion of primary events because ghosts arrive very rapidly after primary events. Within this very short period, the primary events and ghosts become indistinguishable as they overlap with each other. This leads to confusion in determining the actual arrival time of primary events.
2. Broadens the wavelet and deteriorates seismic resolution. Hence, the geological interpretation based on seismic data with ghost is unreliable.
3. Affects the process which relies on amplitude-frequency analysis and low frequency content, especially seismic inversion process which predicts the lithology and fluid content away from the exploration well.

The proximity of ghosts relative to primary events is shown in Figure 1.3 which accounts for the mirror source and receiver models that incorporate additional distance travelled by ghosts. Using trigonometry, the receiver ghost (RG) and source ghost (SG) have travel lag time of t_r and t_s respectively compared to signal and are given by:

$$t_r = \frac{2Z_g (\cos \theta)}{c} \quad (1)$$

$$t_s = \frac{2Z_g (\cos \theta)}{c} \quad (2)$$

where c is the water velocity, which ranges from 1500ms^{-1} to 1540ms^{-1} . The travel lag time of source-receiver ghost (SRG) is the addition of t_r and t_s . Typically t_r and t_s have values less than 20ms and hence the receiver and source ghost are very near to the primary events.

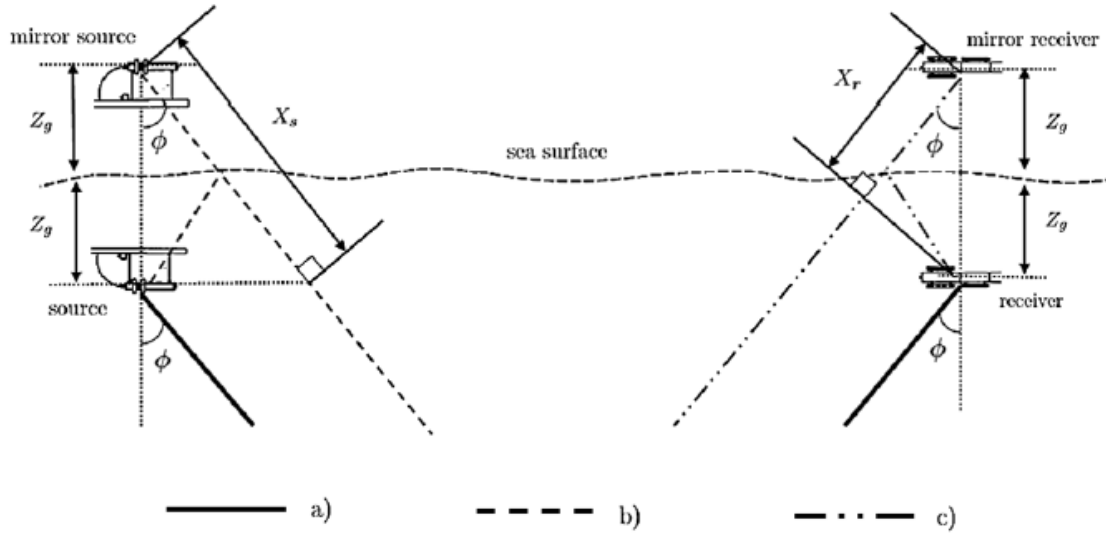


Figure 1.3 Mirror source and receiver models. Z_g is source depth and receiver depth in the left diagram and right diagram respectively. ϕ is the incident angle and emergence angle of signals in the left diagram and right diagram respectively. Event (a), (b) and (c) indicate primary, source ghost and receiver ghost respectively. X_s and X_r represent additional distance travelled by source ghost and receiver ghost respectively. [1]

The distortion and broadening of primary wavelets are explained by the second row of Figure 1.2 which shows the time response of primary and ghosts being recorded by receiver. The receiver ghost (RG) and source ghost (SG) have different polarity with P (primary) because calm water-air interface acts as mirror with reflectivity of -1 and changes the phase of the reflected ghost at the interface by 180° . Negative reflectivity occurs because seawater is denser than air [3]. However, source-receiver ghost (SRG) has the same polarity as primary because it is reflected twice from the sea surface and the reflectivity effect cancels off each other. Since primary signals have different polarity compared to receiver ghost (RG) and source ghost (SG), ghosts distort the amplitude and phase of primary signals, thus causing signals to be broaden and less sharp.

The effect of ghost on amplitude-frequency spectra is best displayed on the third row of Figure 1.2 which shows the amplitude spectrum of the seismic data with and without ghost. The ideal ghostless data shows flat spectrum across all frequency by neglecting the effect of high frequency attenuation by subsurface when the signal travels

deeper. For primary embedded with ghost, the amplitude spectrums are bumpy because the ghost induces constructive and destructive interference repeatedly across the frequency. The ghost overboosts the signals at frequencies where constructive interference occurs. However, notches are introduced by ghost at frequencies where destructive interference occurs. The frequencies where constructive and destructive interference occur are given by f_{max} and f_{min} respectively in the following equations [1]:

$$f_{max} = \frac{c}{2z_g (\cos \phi)} \left(n - \frac{1}{2} \right), n = 0, 1, 2, 3 \dots \quad (3)$$

$$f_{min} = \frac{c}{2z_g (\cos \phi)} (n), n = 0, 1, 2, 3 \dots \quad (4)$$

where c , z_g and ϕ are seawater velocity, source or receiver depth and incident angle or emergence angle of signals respectively. The first notch always occurs at 0Hz irrespective of the source or receiver depth according to the equations above. However, the 0Hz notch is unrecoverable due to the source signature rolloff towards 0Hz and the in-built 0Hz filter in the hydrophones. The source and receiver depths have adverse effect on the amplitude spectrum as shown in Figure 1.4. The shallow tow data has higher frequency and resolution to illuminate thin gas traps and sand layers but suffers from low frequency attenuation and high noise level. Deep tow data has more low frequency content and helps in imaging deep structure such as basalt but suffers from low seismic resolution because the ghost notches occur at middle frequency range of about 30Hz to 80Hz [1]. Furthermore, seismic data which is deeper and recorded further from source location has lower incident angle, thus causing the notch to shift to lower frequency according to the above equations [4].

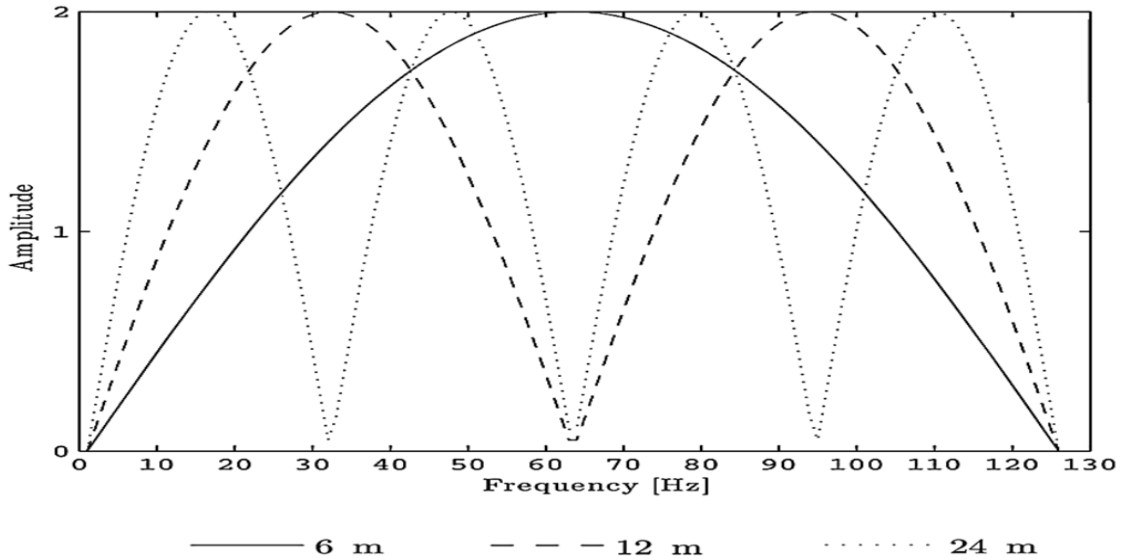


Figure 1.4 Ghost notches introduced by different source or receiver depths [1]

The distortion of amplitude spectrum, especially attenuation at lower frequency below 10Hz, has an adverse effect on seismic inversion process. This is because seismic inversion requires low frequency input from seismic data so that it can predict p-impedance deterministically across subsurface. Otherwise, the low frequency component has to be obtained via well-log interpolation which is inaccurate across subsurface because well log has poor spatial resolution. The unsatisfactory result of seismic inversion imposes higher risks and less confidence in drilling production well in the vicinity of exploration well because the p-impedance contrast between hydrocarbon layer and non-producing layers is less accurate. In conclusion, ghosts are affecting every stage of hydrocarbon exploration, ranging from seismic processing up to drilling of production well.

1.3 Objective

The objectives of the study in this thesis are:

1. To compare the effectiveness of different deghosting algorithms in eliminating ghost. The algorithms that are going to be tested are deterministic deghosting and adaptive deghosting.
2. To investigate the effect of deghosting on the accuracy of p-impedance contrast prediction. The parameter that dictates the effectiveness of deghosting is sea state while the results of p-impedance contrast prediction are compared with well logs.
3. To investigate the accuracy of seismic inversion in predicting p-impedance contrast at each well location and also hydrocarbon-bearing layers. The hydrocarbon-producing layers are confirmed by oil or gas “shows” recorded by the well logs.

1.4 Hypotheses

The hypotheses based on the objectives are as follow:

1. Adaptive deghosting is expected to provide better deghosting result than deterministic deghosting.
2. The higher the sea state, the better the deghosting result and the closer the p-impedance contrast prediction to the well logs.
3. Seismic inversion is an accurate algorithm in predicting p-impedance contrast at each well location and also hydrocarbon-bearing layers.

1.5 Scope

The scope of this study is as follow:

1. Evaluation of different deghosting algorithm, namely deterministic and adaptive deghosting. The seismic data acquired using latest technology such as continuous seismic shooting, near field hydrophones recording and deep streamer towing will be processed using the state-of-the-art processing workflows such as deblending, deterministic debubble and zero phasing, and last but not least, deghosting. All the processing workflows until depth imaging will be the same except for deghosting algorithm used.
2. Investigation of sea state effect on deghosting result. After the best deghosting algorithm is chosen, all the processing workflows will remain the same as above except that the sea state parameter will be tested to obtain the best sea state parameter that fits into whole seismic data.
3. Execution of seismic inversion algorithm at well location and whole seismic data. Localized seismic inversion at well location provides information on the accuracy of predicted p-impedance contrast at each well. Global seismic inversion covering whole seismic data provides information on presence of hydrocarbon layers across large geological area.

1.6 Significance of Study

The geological area in this study covers Vulcan sub-basin, which is a subset of Bonaparte basin in Timor Sea, North-west Shelf of offshore Western Australia. This sub-basin is a proven hydrocarbon reserve with approximately 357 MMBBL of oil, 31 MMBBL of Condensate, and 1.3 TCF of gas remained to be extracted [5]. Hence, there are numerous explorations and production wells drilled in this region. Those wells provide invaluable information on the geological settings, especially p-impedance contrast between different subsurface Earth layers.

This deghosting study is one of the first in Vulcan sub-basin which provides better insight into geological structure and p-impedance contrast within this region. Thus, this deghosted dataset acts as a primary reference for seismic processing sequences in this

basin. Abundant legacy seismic data without deghosting in Vulcan sub-basin or Bonaparte basin can then be deghosted in the same manner in the future to have a better understanding on the whole basin in terms of p-impedance contrast, thus reducing the field development risk. Reprocessing lower resolution legacy seismic data with optimum deghosting algorithm saves more cost compared to reacquiring higher resolution seismic data because seismic acquisition is much more expensive compared to seismic processing.

Although there are a lot of literatures covering various deghosting algorithm and the superiority of one algorithm compared to another, most of them are considered as academic exercise and less attention is being paid to the proper usage of deghosting software. In the seismic processing industry, geophysicists have to tweak only the most important parameter in deghosting software to obtain satisfactory deghosting result within short time. This is crucial so that geophysicists can pay more attention to other time-consuming seismic processing sequences such as demultiple and seismic imaging. The key parameter for deghosting is known as sea state. Only the effect of sea state on the deghosting result is discussed in this thesis to complement the information of available literatures based on the view point of processing geophysicists. Deterministic and adaptive deghosting is also tested with the same sea state parameter in order to determine which method is more suitable for Vulcan sub-basin.

Since there are abundant wells being drilled at Vulcan sub-basin with different recording lengths and quality, it is important to select the wells that are representative of this region. Once the wells are selected, it will make the geological interpretation and reservoir modeling around Vulcan sub-basin easier in the future. The result of seismic inversion done in the future can be cross-checked across these selected wells.

REFERENCES

1. Arv, HB 2015, *Broadband processing of conventional 3D seismic data for near surface geohazard investigation: A North Sea case study*. Master thesis, Norwegian University of Science and Technology.
2. Maximilian, GS 2015, *Adaptive deghosting of seismic data: A power minimization approach*. Master thesis, ETH Zurich.
3. Hamid, A 2011, *Comparison/sensitivity analysis of various deghosting method*. Master thesis, University of Oslo.
4. Bing, B, Chi, C, Min, Y, Ping, W & Yan, H 2013, 'Ghost effect analysis and bootstrap deghosting application on marine streamer data', in *75th EAGE Conference & Exhibition incorporating SPE EUROPEC 2013*, London.
5. Geoscience Australia, *Vulcan Sub-basin*. Available from <http://www.ga.gov.au/provexplorer/provinceDetails.do?eno=28315>. [2014]
6. Gregg, P & Stian, H 2011, 'An acquisition system that extracts the earth response from seismic data', *First Break*, vol. 29, pp. 81-87.
7. Oscar, CA 2014, *Seismic source deghosting: Application to the Delta 3 source array*. Master thesis, ETH Zurich.
8. Ralf, F & Dirk-Jan van, M 2016, 'Noise transfer in variable-depth streamer deghosting', *Geophysical Prospecting*, no. 12454.
9. Zheng, ZZ, Milos, C, Bing, X & Philip, F 2012, 'Analysis of a broadband processing technology applicable to conventional streamer data', *First Break*, vol. 30, pp. 77-82.
10. Yilmaz, O & Baysal, E 2015, 'An effective ghost removal method for marine broadband seismic data processing', in *77th EAGE Conference & Exhibition 2015*, Madrid.

11. Ekeabino, M, David, H, Ralf, F & Satish, S 2016, 'Low frequency signal enhancement by pseudo- V_z deghosting', *First Break*, vol. 34, pp. 35-43.
12. Berkhout, AJ & Gerrit, B 2015, 'Deghosting by echo-deblending', *Geophysical Prospecting*, no. 12293.
13. Rob, T, Stuart, D, Sergio, G & Williams, RG 2014, 'Evaluation of a broadband marine source', *First Break*, vol. 32, pp. 71-76.
14. Zijian, T & Xander, C 2016, 'Joint up/down decomposition and reconstruction using three-component streamers with or without ghost model: the sampling theory', *Geophysical Prospecting*, no. 12438.
15. Thomas, ALG 2016, *Pressure wavefield deghosting and its effects on amplitudes: A bootstrap deghosting approach for horizontal and non-horizontal streamers*. Master thesis, University of Oslo.
16. Soubaras, R & Dowle, R 2010, 'Variable-depth streamer – a broadband marine solution', *First Break*, vol. 28, pp. 89-96.
17. Fabrice, M, Beng, SO, Chu-Ong, T, Sabaresan, M, Tony, H & Yunfeng, L 2013, 'Broadband, long-offset, full-azimuth, staggered marine acquisition in the Gulf of Mexico', *First Break*, vol. 31, pp. 125-132.
18. Amundsen, L & Zhou, H 2013, 'Low-frequency seismic deghosting', *Geophysics*, vol. 78, no. 2, pp. 15-20.
19. Telling, R, Riddalls, N, Azmi, A, Grion, S & Williams, RG 2014, 'Broadband, processing of West of Shetland data', *First Break*, vol. 32, pp. 97-103.
20. Ozdemir, H 2009, 'Unbiased deterministic seismic inversion: more seismic, less model', *First Break*, vol. 27, pp. 43-50.
21. Castillo, G, Mayer, R, Fonseca, P, Coronado, M, Marin, C, Casana, E, Firth, J, Hembd, J, Goss, T, Chu-Ong, T, Vidal, MM, Vazquez, ET & Quiroz, FF 2015, 'Combining BroadSeis 3D HD-WAZ data in a reservoir-driven processing approach for field development', *First Break*, vol. 33, pp. 51-57.
22. Firth, J, Horstad, I & Schakel, M 2014, 'Experiencing the full bandwidth of energy from exploration to production with the art of BroadSeis', *First Break*, vol. 32, pp. 89-97.

23. Saunders, M, Geiger, L, Negri, D, Stein, JA, Sansal, TA & Springman, J 2015, 'Improved stratigraphic interpretation using broadband processing – Sergipe Basin, Brazil', *First Break*, vol. 33, pp. 87-93.
24. Duval, G 2012, 'How broadband can unlock the remaining hydrocarbon potential of the North Sea', *First Break*, vol. 30, pp. 85-91.
25. Moise, G, Body, G, Durussel, V, Mandroux, F & Firth, J 2012, 'UKCS Cornerstone: a variable-depth streamer acquisition case study', *First Break*, vol. 30, pp. 91-98.
26. Ziolkowski, A, Hanssen, P, Gatliff, R, Jakubowicz, H, Dobson, A, Hampson, G, Xiang-Yang, L & Enru, L 2003, 'Use of low frequencies for sub-basalt imaging', *Geophysical Prospecting*, vol. 51, pp 169-182.
27. Hollingworth, S, Pape, O, Purcell, C, Kaszycka, E, Baker, T, Cowley, J, Duval, G & Twigger, L 2015, 'Setting new standards for regional understanding – mega-scale broadband PSDM in the North Sea', *First Break*, vol. 33, pp. 75-79.
28. Carmo, S, Azevedo, L & Soares, A 2017, 'Exploring seismic inversion methodologies for non-stationary geological environments: a benchmark study between deterministic and geostatistical seismic inversion', *Geophysical Prospecting*, no. 12489.
29. Grana, D, Xiaozheng, L & Wenting, W 2016, 'Statistical facies classification from multiple seismic attributes: comparison between Bayesian classification and expectation-maximization method and application in petrophysical inversion', *Geophysical Prospecting*, no. 12428.
30. Naeini, EZ, Gunning, J & White, R 2016, 'Well tie for broadband seismic data', *Geophysical Prospecting*, no. 12433.
31. Kawai, WA & Mukerji, T 2016, 'Integrating basin modeling with seismic technology and rock physics', *Geophysical Prospecting*, no. 12343.
32. Ray, AK & Chopra, S 2016, 'Building more robust low-frequency models for seismic impedance inversion', *First Break*, vol. 34, pp. 47-52.
33. Perez, DO, Velis, DR & Sacchi, MD 2017, 'Three-term inversion of prestack seismic data using a weighted $l_{2,1}$ mixed norm', *Geophysical Prospecting*, no. 12500.

34. Butler, E, Mueller, S & Davis, TL 2016, 'Application of time-lapse multi-component seismic inversion to characterize pressure and stimulation in the Niobrara and Codell Reservoirs, Wattenberg Field, Colorado', *First Break*, vol. 34, pp. 69-75.
35. Andy, H 2011, *Practical petrophysics*, Origin Energy Resources Limited.
36. David, N & Westlake, S 2005, 'Vulcan Sub-basin megasurvey, Australia: visualizing the bigger picture', *Tech Link*, vol. 5, no. 1.
37. Geoscience Australia, *Offshore petroleum exploration acreage release*. Available from <<http://www.petroleum-acreage.gov.au/2016/geology/bonaparte-basin/vulcan-sub-basin>>. [2016]
38. Melbana Energy, *Australia – Vulcan Sub-basin exploration*. Available from <<http://www.melbana.com/irm/content/australia-vulcan-sub-basin-exploration.aspx?RID=385>>. [2017]
39. Bounty Oil and Gas NL, *AC/P 32 Vulcan Sub-basin 500 MMboip prospect, Timor Sea, Australia*. Available from <<http://www.bountyoil.com/wp-content/uploads/2014/01/ACP-32-Management-Final-10012014.pdf>>. [2014]
40. Rodriguez, K, Cook, P & Eastwell, D 2016, 'Beyond the Puffin: Applying modern processing workflows in the Vulcan Sub-basin', *Geo Expro*, pp. 28-32.
41. Polarcus, *Cygnus 3D: Multi-Client Seismic Survey, Vulcan Sub-basin, Australia*. Available from <https://www.polarcus.com/media/2112/cygnus-mc3d-datasheet_140418.pdf>. [2016]
42. DownUnder Geosolutions 2017, *Cygnus Multi-Client 3D – Processing Report*. Available from: DownUnder Geosolutions Internal Report. [1 March 2017]
43. Geoscience Australia, *Offshore Petroleum Exploration Acreage Release (Australia 2016): Vulcan Sub-basin*. Available from <<http://www.petroleum-acreage.gov.au/2016/geology/bonaparte-basin/vulcan-sub-basin>>. [2016]